Dielectric properties of strongly coupled hybridized light-matter states

Aleksandr G. Avramenko
aavramen@vivaldi.net

Abstract

The Lorentz oscillator model is applied to a strongly coupled hybridized light-matter state. It is noted that the real part of the index undergoes rapid change in the area of the so-called "dark states." This property of hybridized light-matter states could allow them to function as unorthodox materials in which their absorptive and refractive properties are selectively manipulated. In this manuscript, basic properties of hybrid light-matter states are reviewed. The Lorentz oscillator model is then applied to two types of light-matter states, one formed from a coupling of a single exciton and a single cavity photon, and one formed from coupling two excitons to a cavity photon.

1. Introduction

The interaction of electromagnetic radiation (light) with matter is a fundamental process required to sustain complex life [1]. For example, the conversion of carbon dioxide and water into complex molecules via photosynthesis is hypothesized to have facilitated the evolution of multicellular organisms [1]. There are two limits to light-matter interaction. The "weak" coupling regime in which the interaction of light and matter results in a change in the radiative properties of the states involved, but does not fundamentally alter the physical properties of either state, and the "strong" coupling regime, in which the physical properties of the states, such as the potential energy surface, are altered [2,3]. Strong light-matter coupling occurs when an electromagnetic wave of a certain frequency interacts with a chromophore which resonates at the same frequency. If the chromophore is unable to dissipate the energy faster than it is being exchanged with the photon, strong light-matter coupling may occur [2]. In order to achieve such conditions the photon is typically trapped in a Fabry-Pérot cavity, as seen in Fig 1A. Strong light-matter coupling between two states (one photonic and one excitonic) will result in the appearance of two polaritonic states, as seen in Fig 2B and described in equation (1) [2]. As evident from equation (1), strong coupling hybridizes the photonic and excitonic states, hence they are often simply referred to as hybrid light-matter states. The formation of "dark states" will also occur, which will occupy an area intermediate of the polaritons. The dark states are a superposition of molecular excitons of the chromophore with little optical character. The optical properties of these polariton states have been of some interest to scientists due to their possible uses such as lasing applications, as well as being used as novel tools to alter chemical reactions [4,5].

$$|^{UP}/_{LP}\rangle = \frac{1}{\sqrt{2}}[|e\rangle_e|0\rangle_c \pm |g\rangle_e|1\rangle_c] \tag{1}$$

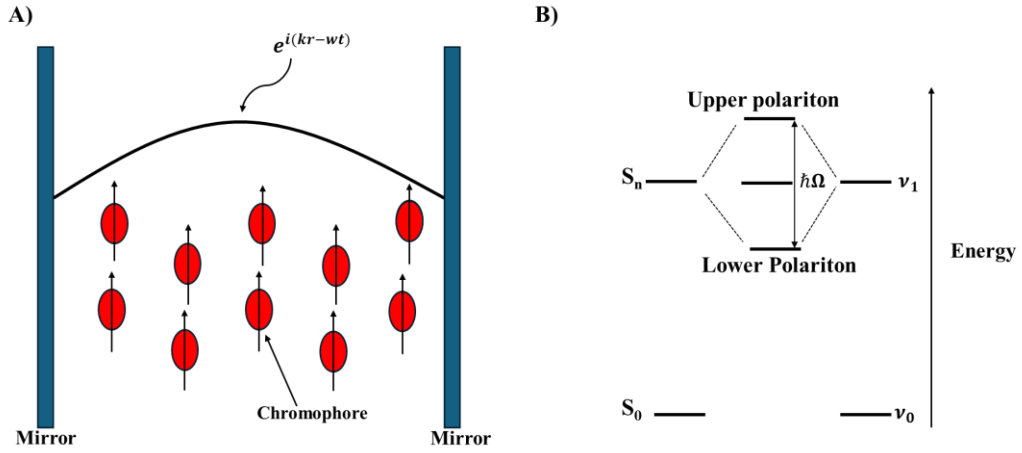

Fig. 1. A) A diagram of a model cavity polariton structure showing an electromagnetic wave being trapped inside a Fabry-Pérot cavity. The light wave is able to interact with a chromophore inside the cavity as it is reflected. B) The energy diagram of a polariton structure. Note that this is similar to the concepts of molecular orbital theory in which two molecular orbitals are created via the interaction of two atomic orbitals.

https://doi.org/10.26434/chemrxiv-2024-lpfs9 **ORCID:** https://orcid.org/0000-0001-5951-0150 Content not peer-reviewed by ChemRxiv. **License:** CC BY-NC-ND 4.0

The two polaritonic states are denoted as the upper polariton (UP) and the lower polariton (LP), as seen in Fig 2B. The two states are separated by an energy referred to as the Rabi splitting ($\hbar\Omega$) [2]. The strong light-matter coupling condition is satisfied by equation (2), where $\hbar\gamma_{ex}^2$ and $\hbar\gamma_{cav}^2$ refer to the full width half maximum (FWHM) of the exciton and the cavity photon respectively [6]. Note that the number of polaritonic states formed is equal to the number of excitonic and photonic states participating in their formation. For simplicity, in Fig. 2B only one of each state is involved. However, strong light-matter coupling involving multiple excitonic states coupled to a single cavity photon have been recorded [7,8]. In such a case, the appearance of additional "middle" polariton states are expected.

$$\hbar\Omega > \sqrt{(\hbar\gamma_{ex}^2 + \hbar\gamma_{cav}^2)/_2} \tag{2}$$

Based on the description in equation (1), it is clear that the wave function of a polariton state is a true hybrid of a photon and an exciton. An oscillator involving a single photon and a single cavity photon can be described by a two-level Hamiltonian, as seen in equation (3), in which the cross-diagonal interaction term in the matrix (*V)* can be estimated by Rabi splitting [9]. Solving for the eigenvalues of the two-level Hamiltonian produces two solutions, as seen in equations (4) & (5), which represent the energies of the UP and LP states. Note that the polariton states are dispersive, the angle at which the Rabi splitting is maximized will be the resonance point of the polariton states, with both UP and LP possessing an equal amount of excitonic and photonic character. It should also be noted that solving for the eigenvectors of equation (3) will result in determining the Hopfield coefficients of each polariton state, which describe their photonic and excitonic characteristics [10]. The Hopfield coefficients can be estimated by equations (6), and (7) [11]. Finally, the imaginary part of equation (3) contains information regarding the FWHM of the polaritonic states. This results in polariton states acquiring a "light-like" character, resulting in the mass and lifetime of the states needing to be corrected for by the Hopfield coefficients [9]. To minimize these possible complications the cavity mode is typically made to have a FWHM similar to that of the exciton that is being coupled to, and experiments are typically performed near resonance, where the photonic and excitonic characters are equal [2].

$$\begin{bmatrix} E_{ex} + i\sigma_{ex} & V \\ V & E_{ph} + i\sigma_{ph} \end{bmatrix} \begin{bmatrix} \alpha \\ \beta \end{bmatrix} = \epsilon \begin{bmatrix} \alpha \\ \beta \end{bmatrix} \tag{3}$$

$$E_{UP(\theta)} = \frac{E_{ph(\theta)} + i\sigma_{ph} + E_{ex} + i\sigma_{ex}}{2} + \frac{1}{2}\sqrt{\left[(E_{ex} + i\sigma_{ex}) - (E_{ph(\theta)} - i\sigma_{ph})\right]^2 + 4V^2} \tag{4}$$

$$E_{LP(\theta)} = \frac{E_{ph(\theta)} + i\sigma_{ph} + E_{ex} + i\sigma_{ex}}{2} - \frac{1}{2}\sqrt{\left[(E_{ex} + i\sigma_{ex}) - (E_{ph(\theta)} - i\sigma_{ph})\right]^2 + 4V^2} \tag{5}$$

$$c_{ph(lp)} = \frac{V^2}{V^2 + (E_{LP(\theta)} - E_{ph(\theta)})^2} \tag{6}$$

$$c_{ph(up)} = \frac{V^2}{V^2 + (E_{UP(\theta)} - E_{ph(\theta)})^2} \tag{7}$$

While equation (3) does well in describing the energy and dispersive behavior of polariton states, it is possible to closely approximate their behavior using classical optical methods. In particular, when describing the behavior of light inside a Fabry-Pérot cavity the wave-transfer matrix can be evoked [12,13]. The wave-transfer matrix, seen in equation (8) relies on using the Fresnel equations for reflectance and transmittance across each boundary involved in constructing the Fabry-Pérot cavity to estimate the final transmittance (or reflectance). Absorption can be simulated within the matrix by adjusting the attenuation coefficient within the layer that possesses the chromophore. This manuscript takes advantage of the fact that the behavior of light inside of a cavity is well approximated by classical methods, utilizing the Lorentz oscillator model to plot out the refractive index of the polariton states.

https://doi.org/10.26434/chemrxiv-2024-lpfs9 **ORCID:** https://orcid.org/0000-0001-5951-0150 Content not peer-reviewed by ChemRxiv. **License:** CC BY-NC-ND 4.0

$$M = \begin{bmatrix} t_{12}t_{21} - r_{12}r_{21} & \frac{r_{21}}{t_{12}} \\ \frac{r_{12}}{t_{21}} & \frac{1}{t_{12}} \end{bmatrix} \tag{8}$$

While the derivation of the Lorentz oscillator model is beyond the scope of this manuscript, the basic principles of it will be explained. In summary, the electromagnetic field is modeled as, $e^{i(kr-wt)}$. When an electromagnetic field interacts with matter two assumptions are made, 1) the charges in the material will possess some inherent oscillating frequency and 2) the charges will resist the electromagnetic field in the opposite direction, in essence the model treats the charges within the material interacting with the electromagnetic field as small springs [14-16]. Already evident from this simple treatment, it should appear clear that due to the complex nature of the electromagnetic field, the Lorentz oscillator model will contain a real, and an imaginary component. The former representing refractance, while the latter attenuation.

2. Results and Discussion

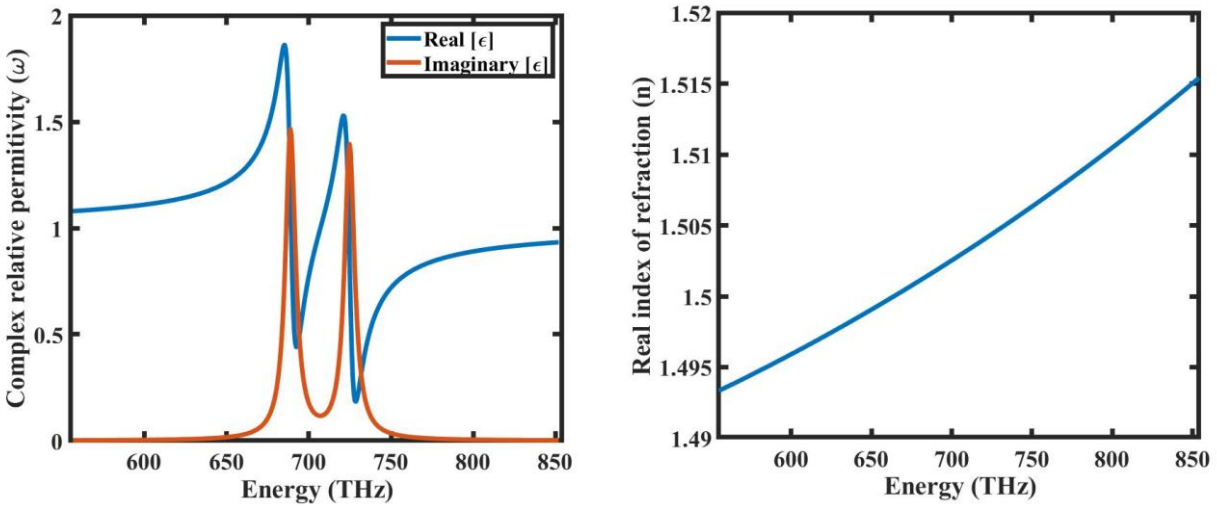

Fig. 2. A) The real and imaginary parts of the index of refraction plotted for a hybrid light-matter state. B) The refractive index of poly methyl methacrylate (PMMA), as calculated using the Sellmeier equation.

$$1 + \left(\frac{\omega_P}{\omega_o^2 - i\gamma\omega - \omega^2}\right)_{UP} + \left(\frac{\omega_P}{\omega_o^2 - i\gamma\omega - \omega^2}\right)_{LP} \tag{9}$$

The Lorentz oscillator model utilized to model the behavior of the complex index of refraction is provided in equation (9). The UP and LP notation denotes the upper and lower polariton. The total index can be modeled as a sum of each individual component [16]. In equation (9) ω_P refers to the plasma frequency, which was set at ω_P=1000γ. The excitonic resonance frequency,ω_o^2, was set to 688.9 THZ for the LP and 724.8 THz for the UP. The damping component γ was set at 7.451 THz. These values are estimates based on a polariton model formed by strong light-matter coupling between a cavity photon and a Zinc tetraphenyl porphyrin molecule described in previous literature [5]. The results of equation (9) are plotted in Fig. 2A. In Fig, 2A, the imaginary portion of the index represents attenuation of the electromagnetic field as it passes through a material. The real portion of the index represents the ratio of the phase velocity of the electromagnetic wave traveling through the medium to that of an electromagnetic wave in vacuum [16]. The simple Lorentz oscillator model demonstrates the large rate of change in phase velocity experienced by the real portion of the refractive index near the dark states (706.9 THz).

The Lorentz oscillator model is further applied to a system that contains two excitonic and one photonic state, requiring the modeling of three polariton states, the UP, LP, and a middle polariton (MP), as seen in Fig. 3. In order to accomplish this, equation (9) is simply expanded to accommodate an additional polariton energy level, as seen in equation (10).

$$1 + \left(\frac{\omega_P}{\omega_o^2 - i\gamma\omega - \omega^2}\right)_{UP} + \left(\frac{\omega_P}{\omega_o^2 - i\gamma\omega - \omega^2}\right)_{LP} + \left(\frac{\omega_P}{\omega_o^2 - i\gamma\omega - \omega^2}\right)_{MP} \tag{10}$$

https://doi.org/10.26434/chemrxiv-2024-lpfs9 **ORCID:** https://orcid.org/0000-0001-5951-0150 Content not peer-reviewed by ChemRxiv. **License:** CC BY-NC-ND 4.0

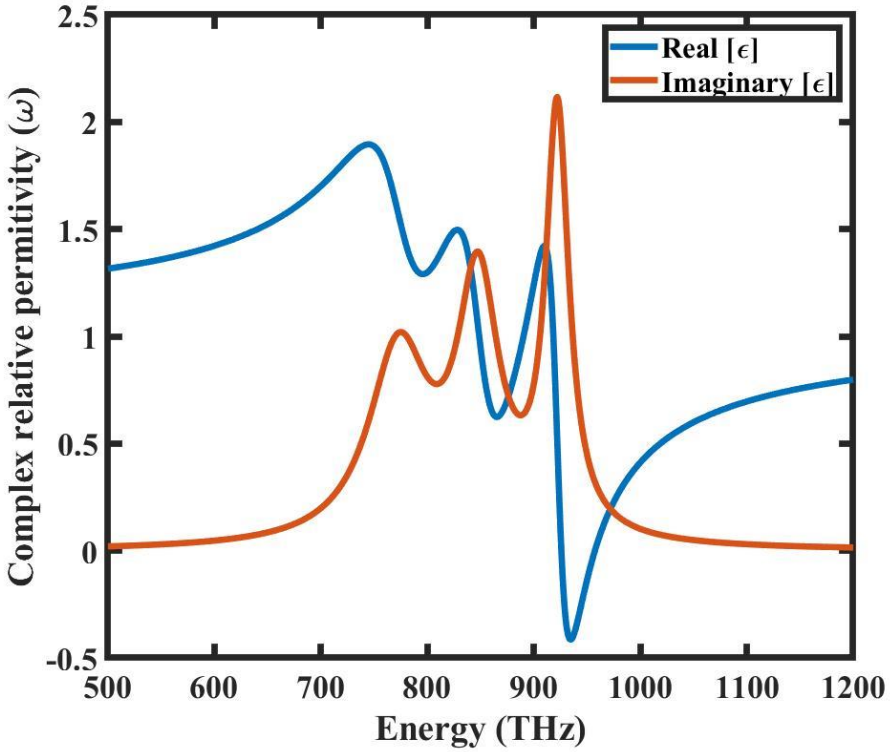

Fig. 3. The real and imaginary parts of the index of refraction plotted for a hybrid light-matter state formed from two excitons and a single cavity photon.

In equation (10) the γ component for the LP was set at 68.9 THz, the LP at 26.3, while the MP was the average of the two values. The resonance frequency ω_o^2 was set at 773.7 for the LP, 922.1 THz for the UP and the average of the two values for the MP. These values were based on work obtained by Forrest *et al.* [7]. Note that while simplistic, at resonance the MP will have an equal amount of contribution from both excitonic states [17]. Therefore, averaging the two excitonic contributions should provide for an estimate of the FWHM of the MP. A strongly light-coupled state formed from two excitons and a single cavity photon results in the real portion of the refractive index undergoing considerable change in the area of the middle polariton, as seen in Fig 3.

$$n^2 - 1 = \frac{0.99654\lambda^2}{\lambda^2 - 0.00787} + \frac{0.18964\lambda^2}{\lambda^2 - 0.02191} + \frac{0.0.00411\lambda^2}{\lambda^2 - 3.85727} \tag{11}$$

The refractive index is dependent on temperature and wavelength, however, the change in the index is often small, or inherent to the physical structure of the material [14,18]. This is visualized in Fig. 2B where the Sellmeier equation is used to estimate the real part of the refractive index for poly methyl methacrylate (PMMA). This polymeric material has been used as a medium to form polaritons due to the precision to which the coating can be made, the Sellmeier equation for PMMA is provided in equation (11) [5,19]. Creating materials whose index can be selectively controlled has been of some interest to scientists [20]. One such path is via the use of acousto-optic devices, in which a sound (acoustic) wave is used to generate a gradient within an optical material. In turn, the electromagnetic field traveling through such a gradient will experience a different refractive index then one without a gradient. In summary, the new transmittance must be calculated using the wave-transfer matrix seen in equation (8). One limitation of using acousto-optic modulators is the need to carefully focus the light unto the crystal in order to get sufficient modulation, while at the same time requiring a source of acoustic waves [21]. Another way the index of refraction of a material can be manipulated is via the photorefractive effect [20]. Unlike sound waves the photorefractive effect relies on utilizing light to manipulate the refractive index of a material. The rapidly changing index of refraction in polaritonic media between the UP and LP states would appear to make them a suitable candidate for a modular optical material. Moreover, unlike acoustic or photorefractive materials currently in use which may require material restrictions, polaritons have been formed from a wide range of materials, such as quantum well semiconductors, as well as molecular and vibronic excitations [22,23]. Finally, polaritons do not require an outside energy source, that is, once strong light-matter hybridization is achieved, a presence of a single

https://doi.org/10.26434/chemrxiv-2024-lpfs9 **ORCID:** https://orcid.org/0000-0001-5951-0150 Content not peer-reviewed by ChemRxiv. **License:** CC BY-NC-ND 4.0

photon trapped in the cavity maintains the polariton states [24]. This property is illustrated by equation (12) which defines Rabi splitting [24,25]. From equation (12), Rabi splitting is based on the resonance energy ($\hbar\omega$), the permittivity of vacuum and the volume of the electromagnetic mode ($\epsilon_0 v$) as well as the dipole moment of the chromophores involved in strong light-matter coupling (*d*). Also, due to the $n_{photon} + 1$ factor, a photon will always be present within the cavity upon polariton formation.

$$\hbar\Omega = 2d\left(\frac{\hbar\omega}{2\epsilon_0 v}\right)^{1/2}\left(n_{photon}+1\right)^{1/2} \tag{12}$$

3. Conclusion

The complex index of refraction of two different materials strongly coupling to a cavity photon was modeled using the Lorentz oscillator model. The model shows a rapid change of the real index of refraction between the polariton states. This property of dark states may allow polaritons to function as a new type of photorefractive materials. For example, polaritons can be incorporated into coatings in order to alter the complex refractive index of the material, allowing the coating to be highly absorbent in areas it would typically lack such a characteristic, or selectively increase transparency in others. While an obvious limitation of such a material would be the need to construct two mirrors to maintain a cavity photon, recent work has been conducted in which polaritons are created by coupling to phonon resonances, which do not require the second mirror [26]. Finally, because the material which holds the chromophores that couple with the cavity photons to form polariton states would expand and contract with temperature changes, the strength of the optical response could be controlled by manipulating the coating's thickness, allowing for a selective manipulation of refractance and absorbance [27].

4. Appendix

Listed below is the MATLAB code used to generate Fig. 2 and 3.

```
clc
close all
clear all
%%
c=2.99*10^8; %light
q_e=1.60217646*10^-10; % coulombs
e_e=8.8541878176*10*10^-12; %faraday
m_e=9.10938188*10^-31; %electron mass
N=6.022*10^23; % Avogadro

v1= 100:1:1500; %scale in THz
v=v1*(10^12); %Hz conversion factor
%% Two oscillator model
Gamma=7.451; %FWHM estimate in THz
Omega=688.9; %LP energy
Omega2=724.8;% UP energy
Height=5637; %peak height for Lorentz equation
Plasma_freq=1000.*Gamma; %Plasma frequency

plot_chi=(((Plasma_freq)./((Omega^2)-(j.*Gamma.*v1)-(v1.^2))));
plot_chi2=1+(((Plasma_freq)./((Omega2^2)-(j.*Gamma.*v1)-(v1.^2))));
chi_combined=plot_chi+plot_chi2; %Combine Lorentz oscillator model

figure
box on
hold on
plot(v1,chi_combined)
plot(v1,imag(chi_combined))
xlabel('Energy (eV)')
ylabel('Complex relative permitivity (\omega)')
legend('Real [\epsilon]','Imaginary [\epsilon]')
xlim([555 854])
%% Three oscillator model
GammaUP=26.3;
GammaLP=68.9;
GammaMP=(GammaUP+GammaLP)./2;
OmegaUP=922.1;
OmegaLP=773.7;
OmegaMP=(OmegaUP+OmegaLP)./2;
```

https://doi.org/10.26434/chemrxiv-2024-lpfs9 **ORCID:** https://orcid.org/0000-0001-5951-0150 Content not peer-reviewed by ChemRxiv. **License:** CC BY-NC-ND 4.0

```
Height=5637;
Plasma_freq2=1000.*GammaMP;

plot_chi3=(((Plasma_freq2)./((OmegaUP^2)-(j.*GammaUP.*v1)-(v1.^2))));
plot_chi4=(((Plasma_freq2)./((OmegaLP^2)-(j.*GammaLP.*v1)-(v1.^2))));
plot_chi5=(((Plasma_freq2)./((OmegaMP^2)-(j.*GammaMP.*v1)-(v1.^2))));
chi_combined2=1+plot_chi3+plot_chi4+plot_chi5;

figure
box on
hold on
plot(v1,chi_combined2)
plot(v1,imag(chi_combined2))
xlabel('Energy (THz)')
ylabel('Complex relative permitivity (\omega)')
legend('Real [\epsilon]','Imaginary [\epsilon]')
xlim([500 1200])

%% Sellmier for PMMA
F=0.99654;
G=(0.00787);
F1=0.18964;
G1=(0.02191);
F2=0.00411;
G2=(3.85727);
yy=((2.99*10^8)./(v*10^-6));
yy2=(yy).^2;
nn3=((F*yy2)./((yy2)-G));
nn3a=nn3+((F1*yy2)./((yy2)-G1));
nn3b=nn3a+((yy2*F2)/((yy2)-G2));
nindex3=(sqrt((nn3b+1)));

figure
box on
hold on
plot(v1,nindex3)
xlabel('Energy (THz)')
ylabel('Real index of refraction (n)')
xlim([555 854])
```

5. Acknowledgements

This work is dedicated to the memory of Anna Avramenko.

References

[1] B. E. Schirrmeister, J.M. de Vos, A.Antonelli, and H.C. Bagheri, “Evolution of multicellularity coincided with increased diversification of cyanobacteria and the Great Oxidation Event,” *PNAS*, vol. 110, no. 5, pp. 1791-1796, 2013, https://doi.org/10.1073/pnas.1209927110
[2] T. W. Ebbesen, “Hybrid light-matter states in a molecular and material science perspective,” *Accounts of chemical research*, vol. 49, no. 11, pp. 2403-2412, 2016, https://doi.org/10.1021/acs.accounts.6b00295
[3] J. Feist, J. Galego, Javier F.J. Garcia-Vidal, “Polaritonic Chemistry with Organic Molecules,” *ACS Photonics*, vol 5, no. 1, pp. 205-216, 2018, https://doi.org/10.1021/acsphotonics.7b00680
[4] S. Kéna-Cohen, S. R. Forrest, “Room-temperature polariton lasing in an organic single-crystal microcavity,” *Nature*, vol. 4, no. 6, pp. 371-375, 2010, https://doi.org/10.1038/nphoton.20
[5] A. G. Avramenko, A. S. Rury, “Local molecular probes of ultrafast relaxation channels in strongly coupled metalloporphyrin-cavity systems,” *The Journal of Chemical Physics*, vol. 155, no. 6, pp. 064702-1, 2021, https://doi.org/10.1063/5.0055296
[6] J. Wang, R. Su, J. Xing, D. Bao, C. Diederichs, S. Liu,T.C.H. Liew, Z. Chen, Q. Xiong,” Room Temperature Coherently Coupled Exciton−Polaritons in Two-Dimensional Organic−Inorganic Perovskite,” *ACS Nano*, vol. 12, no. 8, pp. 8382—8389, 2018, https://doi.org/10.1021/acsnano.8b03737
[7] M. Slootsky, X. Liu, V. Menon, S. R. Forrest, “Room Temperature Frenkel-Wannier-Mott Hybridization of Degenerate Excitons in a Strongly Coupled Microcavity,” *Physical Review Letters*, vol 112, no. 7, pp. 076401, 2014, https://doi.org/10.1103/PhysRevLett.112.076401
[8] R. J. Holmes, S. R. Forrest, “Strong Exciton-Photon Coupling and Exciton Hybridization in a Thermally Evaporated Polycrystalline Film of an Organic Small Molecule,” *Physical Review Letters*, vol 93, no. 18, pp. 186404, 2004, https://doi.org/10.1103/PhysRevLett.93.186404
[9] D. Bajoni, “Polariton lasers. Hybrid light–matter lasers without inversion,” *Journal of Physics D: Applied Physics*, vol. 45, no 40, pp. 409501, 10.1088/0022-3727/45/40/409501
[10] J.J. Hopfield, “Theory of the Contribution of Excitons to the Complex Dielectric Constant of Crystals”, *Physical Review*., vol. 112, no. 5, pp. 1555, (1958), https://doi.org/10.1103/PhysRev.112.1555
[11] A. Graf, Strong light-matter interactions and exciton-polaritons in carbon nanotubes, Heidelberg University, Department of Physical Chemistry, Ph.D. Dissertation, DOI: 10.11588/heidok.00026454
[12] E. A. Saleh, M. C. Teich, “Fundamental of Optics and Photonics,” Wiley, 2007, 2nd ed. Chap. 10.
[13] A. Avramenko, “Photophysics Of Metalloporphyrins Strongly Coupled To Cavity Photons,” Wayne State University-Department of Chemistry, Ph.D. Dissertation.
[14] J. Peatross, M. Ware, “Physics of Light and Optics,” Bringham Young University, 2024, Chap. 2.

https://doi.org/10.26434/chemrxiv-2024-lpfs9 **ORCID:** https://orcid.org/0000-0001-5951-0150 Content not peer-reviewed by ChemRxiv. **License:** CC BY-NC-ND 4.0

[15] A. B. Djurišić, E. Herbert Li, "Modeling the index of refraction of insulating solids with a modified lorentz oscillator model," *Applied optics*, vol. 37, no 22, pp. 5291-5297, 1998, https://doi.org/10.1364/AO.37.005291
[16] R. P. Feynman, "The Feynman lectures on physics," (Addison–Wesley, 1964), vol 2, Chap. 1.
[17] M. Wang, M. Hertzog, K. Börjesson, "Polariton-assisted excitation energy channeling in organic heterojunctions," *Nature*, vol. 12, no. 1, pp. 1874, 2021, https://doi.org/10.1038/s41467-021-22183-3
[18] A. D. Rakić, "Algorithm for the determination of intrinsic optical constants of metal films: application to aluminum," *Applied Optics*, vol. 34, no. 22, pp. 4755-4767, 1995, https://doi.org/10.1364/AO.34.004755
[19]R. Blümel, M. Bagcioglu, R. Lukacs, A. Kohler, "Infrared refractive index dispersion of polymethyl methacrylate spheres from mie ripples in fourier-transform infrared microscopy extinction spectra," *Journal of the Optical Society of America A*, vol. 33, no. 9, pp. 1687–1696, 2016, https://doi.org/10.1364/JOSAA.33.001687
[20] T.J. Hall, R. Jaura, L.M. Connors, P.D. Foote, "The photorefractive effect—a review," *Progress in Quantum Electronics*, vol. 10, no. 2, pp. 77-146, 1985, https://doi.org/10.1016/0079-6727(85)90001-1
[21] M. Duocastella, S. Surdo, A. Zunino, A. Diaspro, P. Saggau, "Acousto-optic systems for advanced microscopy," *Journal of Physics: Photonics*, vol. 3, no. 1, pp. 012004, 2020, https://doi.org/10.1088/2515-7647/abc23c
[22] R. André, D. Heger, L. S. Dang, Y. M. d'Aubigné, "Spectroscopy of polaritons in CdTe-based microcavities," *Journal of Crystal Growth*, vol. 184, pp. 758-762, 1998, https://doi.org/10.1016/S0022-0248(98)80158-9
[23] A. Thomas, A. Jayachandran, L. Lethuillier-Karl, R. M.A. Vergauwe , K. Nagarajan, E. Devaux, C. Genet, J. Moran, T. W. Ebbesen, "Ground state chemistry under vibrational strong coupling: dependence of thermodynamic parameters on the Rabi splitting energy," *Nanophotonics*, vol. 9 no. 2, pp. 249-255, 2020, https://doi.org/10.1515/nanoph-2019-0340
[24] E. Orgiu, J. George, J. A. Hutchison, E. Devaux, J. F. Dayen, B. Doudin, F. Stellacci, C. Genet, J. Schachenmayer, C. Genes, G. Pupillo, P. Samorì, T. W. Ebbesen, "Conductivity in organic semiconductors hybridized with the vacuum field," *Nature*, vol. 14, no. 11, pp. 1123—1129, 2015, https://doi.org/10.1038/nmat4392
[25] D. G. Lidzey, D. D. C. Bradley, M. S. Skolnick, T. Virgili, S. Walker, D. M. Whittaker, "Strong exciton-photon coupling in an organic semiconductor microcavity," *Nature*, vol. 395, no. 6697, pp. 53-55, 1998, https://doi.org/10.1038/25692
[26] A.M. Berghuis, A. Halpin, Q. Le-Van, M. Ramezani, S. Wang, S. Murai, J. Gómez Rivas, "Enhanced Delayed Fluorescence in Tetracene Crystals by Strong Light-Matter Coupling," *Advanced Functional Materials*, vol. 29, no. 36, pp. 1901317, 2019, https://doi.org/10.1002/adfm.201901317
[27] O. Čip, R. Šmíd , M. Čížek , Z. Buchta, J. Lazar, "Study of the thermal stability of Zerodur glass ceramics suitable for a scanning probe microscope frame," *Central European Journal of Physics*, vol. 10, pp. 447-453, 2012, https://doi.org/10.2478/s11534-011-0112-6

https://doi.org/10.26434/chemrxiv-2024-lpfs9 **ORCID:** https://orcid.org/0000-0001-5951-0150 Content not peer-reviewed by ChemRxiv. **License:** CC BY-NC-ND 4.0